
Fast Bayesian Optimization of Machine Learning Hyperparameters on Large Datasets

Aaron Klein, Stefan Falkner
 Department of Computer Science
 University of Freiburg
 {kleinaa, sfalkner}
 @cs.uni-freiburg.de

Simon Bartels, Philipp Hennig
 Department of Empirical Inference
 Max Planck Institute for Intelligent Systems
 {simon.bartels, phennig}
 @tuebingen.mpg.de

Frank Hutter
 Department of Computer Science
 University of Freiburg
 fh@cs.uni-freiburg.de

Abstract

Bayesian optimization has become a successful tool for hyperparameter optimization of machine learning algorithms, such as support vector machines or deep neural networks. But it is still costly if each evaluation of the objective requires training and validating the algorithm being optimized, which, for large datasets, often takes hours, days, or even weeks. To accelerate hyperparameter optimization, we propose a generative model for the validation error as a function of training set size, which is learned during the optimization process and allows exploration of preliminary configurations on small subsets, by extrapolating to the full dataset. We construct a Bayesian optimization procedure, dubbed FABOLAS, which models loss and training time as a function of dataset size and automatically trades off high information gain about the global optimum against computational cost. Experiments optimizing support vector machines and deep neural networks show that FABOLAS often finds high-quality solutions 10 to 100 times faster than other state-of-the-art Bayesian optimization methods.

1 Introduction

The performance of many machine learning algorithms hinges on certain hyperparameters. For example, the prediction error of non-linear support vector machines depends on regularization and kernel hyperparameters C and γ ; and modern neural networks are sensitive to a wide range of hyperparameters, including learning rates, momentum terms, number of units per layer, dropout rates, weight decay, etc. [1]. The poor scaling of naïve methods like grid search with dimensionality has driven interest in more sophisticated hyperparameter optimization methods over the past years [2, 3, 4, 5, 6, 7, 8, 9, 10, 11]. *Bayesian optimization* has emerged as an efficient framework, achieving impressive successes. For example, in several studies, it found better instantiations of convolutional network hyperparameters than domain experts, repeatedly improving the top score on the CIFAR-10 [12] benchmark without data augmentation [5, 13, 11].

In the traditional setting of Bayesian hyperparameter optimization, the loss of a machine learning algorithm with hyperparameters $\mathbf{x} \in \mathbb{X}$ is treated as the “black-box” problem of finding $\arg \min_{\mathbf{x} \in \mathbb{X}} f(\mathbf{x})$, where the only mode of interaction with the objective f is to evaluate it for inputs $\mathbf{x} \in \mathbb{X}$. If individual evaluations of f on the entire dataset require days or weeks, only very few evaluations are possible, limiting the quality of the best found value. Human experts instead often study performance on

subsets of the data first, to become familiar with its characteristics before gradually increasing the subset size [14, 1]. This approach can still outperform contemporary Bayesian optimization methods.

Motivated by this expert strategy, here we leverage dataset size as an additional degree of freedom enriching the representation of the optimization problem. We treat the dataset size s as an additional input to the blackbox function, and allow the optimizer to actively choose it at each function evaluation. This allows Bayesian optimization to mimic and improve upon human experts when exploring the hyperparameter space. Since s is not a hyperparameter itself, though, the goal of optimization remains good performance on the full dataset, i.e. for the maximal value of s .

Hyperparameter optimization for large datasets has been explored by other authors before. Our approach is similar to Multi-Task Bayesian optimization by Swersky et al. [8], where knowledge is transferred between a finite number of correlated tasks. If these tasks represent manually-chosen subset-sizes, this method also tries to find the best configuration for the full dataset by evaluating smaller, cheaper subsets. However, the discrete nature of tasks in that approach requires evaluations on the entire dataset to learn the necessary correlations. Instead, our approach exploits regularity of performance across dataset size, enabling generalization to the full set without evaluating it directly.

Other approaches for hyperparameter optimization on large datasets include recent work by Nickson et al. [15], who estimated a configuration’s performance on a large dataset by evaluating several training runs on small, random subsets of fixed, manually-chosen sizes. Krueger et al. [16] showed that in practical applications small subsets can suffice to estimate a configuration’s quality, and proposed a cross-validation scheme that sequentially tests a fixed set of configurations on a growing subset of the data, discarding poorly-performing configurations early.

In §2 we review Bayesian optimization, in particular the Entropy Search algorithm and the related method of Multi-Task Bayesian optimization. In §3, we introduce our new Bayesian optimization method FABOLAS for hyperparameter optimization on large datasets. It uses Entropy Search to, at each time step, choose the configuration \mathbf{x} and dataset size s predicted to yield most information about the loss-minimizing configuration on the full dataset *per unit time spent*. In §4, a broad range of experiments with support vector machines and various deep neural networks show that FABOLAS often identifies good hyperparameter settings 10 to 100 times faster than state-of-the-art Bayesian optimization methods acting on the full dataset.

2 Bayesian optimization

Given a black-box function $f : \mathbb{X} \rightarrow \mathbb{R}$, Bayesian optimization¹ aims to find an input $\mathbf{x}_* \in \arg \min_{\mathbf{x} \in \mathbb{X}} f(\mathbf{x})$ that globally minimizes f . It requires a prior $p(f)$ over the function and an acquisition function $a_{p(f)} : \mathbb{X} \rightarrow \mathbb{R}$ quantifying the *utility* of an evaluation at any \mathbf{x} . With these ingredients, the following three steps are iterated [17]: (1) find the most promising $\mathbf{x}_{n+1} \in \arg \max_{\mathbf{x}} a_p(\mathbf{x})$ by numerical optimization; (2) evaluate the expensive and often noisy function $y_{n+1} \sim f(\mathbf{x}_{n+1}) + \mathcal{N}(0, \sigma^2)$ and add the resulting data point $(\mathbf{x}_{n+1}, y_{n+1})$ to the set of observations $\mathcal{D}_n = (\mathbf{x}_j, y_j)_{j=1 \dots n}$; and (3) update $p(f | \mathcal{D}_{n+1})$ and $a_{p(f | \mathcal{D}_{n+1})}$. Typically, evaluations of the acquisition function a are cheap compared to evaluations of f such that the optimization effort is negligible.

2.1 Gaussian Processes

Gaussian processes (GP) are a prominent choice for $p(f)$, thanks to their descriptive power and analytic tractability [e.g. 19]. Formally, a GP is a collection of random variables, any linear finite projection of which is jointly Gaussian distributed. A GP is identified by a mean function m (often set to $m(\mathbf{x}) = 0 \ \forall \mathbf{x} \in \mathbb{X}$), and a positive definite covariance function (kernel) k . Given observations $\mathcal{D}_n = (\mathbf{x}_j, y_j)_{j=1 \dots n} = (\mathbf{X}, \mathbf{y})$ with joint Gaussian likelihood $p(\mathbf{y} | \mathbf{X}, f(\mathbf{X})) = \mathcal{N}(\mathbf{y}; f(\mathbf{X}), \Sigma)$, the posterior $p(f | \mathcal{D}_n)$ is also a GP, with mean and covariance functions of simple analytic form.

The covariance function is the core object determining how observations influence predictions. Below we will construct a custom-designed covariance over dataset sizes. Along the other dimensions, we adopt the Matérn $5/2$ kernel [20], in its Automatic Relevance Determination form [21]. This is a relatively standard choice in the Bayesian optimization literature, a stationary, twice-differentiable model, which is preferable to the Gaussian kernel popular elsewhere, because it makes less restrictive

¹Comprehensive tutorials are presented by Brochu et al. [17] and Shahriari et al. [18].

smoothness assumptions, which can be helpful in the optimization setting [5]:

$$k_{5/2}(\mathbf{x}, \mathbf{x}') = \theta \left(1 + \sqrt{5} d_{\lambda}(\mathbf{x}, \mathbf{x}') + 5/3 d_{\lambda}^2(\mathbf{x}, \mathbf{x}') \right) e^{-\sqrt{5} d_{\lambda}(\mathbf{x}, \mathbf{x}')} . \quad (1)$$

Here, θ and λ are free parameters—hyperparameters of the GP surrogate model—and $d_{\lambda}(\mathbf{x}, \mathbf{x}') = (\mathbf{x} - \mathbf{x}')^{\top} \text{diag}(\lambda)(\mathbf{x} - \mathbf{x}')$ is the Mahalanobis distance. An additional hyperparameter of the GP model is the noise covariance σ^2 in the likelihood $p(\mathbf{y} \mid \mathbf{X}, f(\mathbf{X}))$ above. For clarity: These GP hyperparameters are *internal* hyperparameters of the Bayesian optimizer, as opposed to those of the target machine learning algorithm to be tuned.

2.2 Acquisition functions

The role of the acquisition function is to trade off exploration vs. exploitation. Popular choices include Expected Improvement (EI) [22], Upper Confidence Bound (UCB) [23], Entropy Search (ES) [24], and Predictive Entropy Search (PES) [25]. In our experiments, we will use EI and ES. We found EI to perform robustly in most applications, providing a solid baseline; it is defined as

$$a_{\text{EI}}(\mathbf{x} \mid \mathcal{D}_n) = \mathbb{E}_p[\max(f_{\min} - f(\mathbf{x}), 0)] . \quad (2)$$

where f_{\min} is the best function value known (also called the *incumbent*). This expected drop over the best known value is high for points predicted to have small mean and/or large variance.

ES is a more recent acquisition function that selects evaluation points based on the predicted *information gain* about the optimum, rather than aiming to evaluate near the optimum. At the heart of ES lies the probability distribution $p_{\min}(\mathbf{x} \mid \mathcal{D}) := p(\mathbf{x} \in \arg \min_{\mathbf{x}' \in \mathbb{X}} f(\mathbf{x}') \mid \mathcal{D})$, the belief about the function’s minimum given the prior on f and observations \mathcal{D} . The *information gain* at \mathbf{x} is then measured by the expected Kullback-Leibler divergence (relative entropy) between $p_{\min}(\cdot \mid \mathcal{D} \cup \{(\mathbf{x}, y)\})$ and the uniform distribution $u(\mathbf{x})$, with expectations taken over the measurement y to be obtained at \mathbf{x} :

$$a_{\text{ES}}(\mathbf{x}) := \mathbb{E}_{p(y \mid \mathbf{x}, \mathcal{D})} \left[\int p_{\min}(\mathbf{x}' \mid \mathcal{D} \cup \{(\mathbf{x}, y)\}) \cdot \log \frac{p_{\min}(\mathbf{x}' \mid \mathcal{D} \cup \{(\mathbf{x}, y)\})}{u(\mathbf{x}')} d\mathbf{x}' \right] . \quad (3)$$

The primary numerical challenge in this framework is the computation of $p_{\min}(\cdot \mid \mathcal{D} \cup \{(\mathbf{x}, y)\})$ and the integral above. Due to the intractability, several approximations have to be made. We refer to Hennig and Schuler [24] for details, as well as to the supplemental material (Section A), where we also provide pseudocode for our implementation. Despite the conceptual and computational complexity of ES, it offers a well-defined concept for information gained from function evaluations, which can be meaningfully traded off against other quantities, such as the evaluations’ cost.

PES refers to the same acquisition function, but uses different approximations to compute it. In our experience ES and PES perform comparably, and in Section 3.4 we describe why for our application ES was the more direct choice.

2.3 Multi-Task Bayesian optimization

We briefly review the *Multi-Task* Bayesian optimization (MTBO) method of Swersky et al. [8], which is closely related to our approach. Given a set of tasks $\mathbb{T} = \{1, \dots, T\}$, the objective function $f : \mathbb{X} \times \mathbb{T} \rightarrow \mathbb{R}$ corresponds to evaluating a given $\mathbf{x} \in \mathbb{X}$ on one of the tasks $t \in \mathbb{T}$. The relation between points in $\mathbb{X} \times \mathbb{T}$ is modeled via a GP using a product kernel:

$$k_{\text{MT}}((\mathbf{x}, t), (\mathbf{x}', t')) = k_T(t, t') \cdot k_{5/2}(\mathbf{x}, \mathbf{x}') . \quad (4)$$

The kernel k_T is represented implicitly by the Cholesky decomposition of $k(\mathbb{T}, \mathbb{T})$ whose entries are sampled via MCMC together with the other hyperparameters of the GP. By considering the distribution of the optimum on a target task $t_* \in \mathbb{T}$, $p_{\min}^{t_*}(\mathbf{x} \mid \mathcal{D}) := p(\mathbf{x} \in \arg \min_{\mathbf{x}' \in \mathbb{X}} f(\mathbf{x}', t = t_*) \mid \mathcal{D})$, and computing any information w.r.t. it, Swersky et al. [8] use the information gain per unit cost as their acquisition function²:

$$a_{\text{MT}}(\mathbf{x}, t) := \frac{\mathbb{E}_{p(y \mid \mathbf{x}, t, \mathcal{D})} \left[\int p_{\min}^{t_*}(\mathbf{x}' \mid \mathcal{D} \cup \{(\mathbf{x}, t, y)\}) \cdot \log \frac{p_{\min}^{t_*}(\mathbf{x}' \mid \mathcal{D} \cup \{(\mathbf{x}, t, y)\})}{u(\mathbf{x}')} d\mathbf{x}' \right]}{c(\mathbf{x}, t)} . \quad (5)$$

²In fact, Swersky et al. [8] deviated slightly from this formula (which follows the ES approach of [24]) by considering the difference in information gains in $p_{\min}^{t_*}(\mathbf{x} \mid \mathcal{D})$ and $p_{\min}^{t_*}(\mathbf{x} \mid \mathcal{D} \cup \{(\mathbf{x}, y)\})$. They stated this to work better in practice, but we did not find evidence for this in our experiments and thus, for consistency, use the variant presented here throughout.

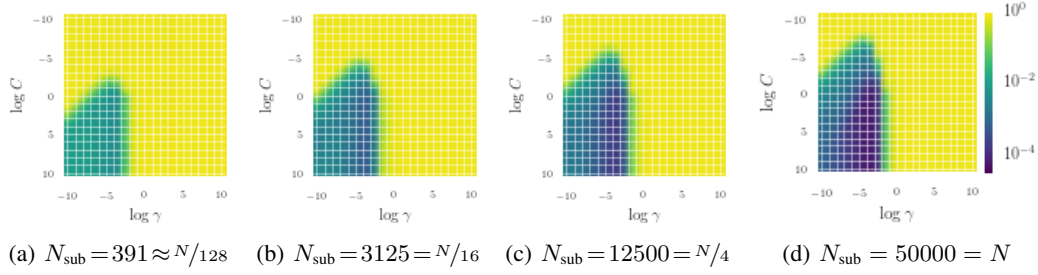


Figure 1: Validation error of a grid of 400 SVM configurations (20 settings of each of the regularization parameter C and kernel parameter γ , both on a log-scale in $[-10, 10]$) for subsets of the MNIST dataset [27] of various sizes N_{sub} . Small subsets are quite representative: The validation error of bad configuration (yellow) remains constant at around 0.9, whereas the region of good configurations (blue) does not change drastically with N_{sub} .

The numerator represents the information gain on the target task averaged over the possible outcomes of $f(\mathbf{x}, t)$. If the cost $c(\mathbf{x}, t)$ of a configuration \mathbf{x} on task t is not known a priori it can be modelled the same way as the objective function.

This model supports machine learning hyperparameter optimization for large datasets by using discrete dataset sizes as tasks. Swersky et al. [8] indeed studied this approach for the special case of $\mathbb{T} = \{0, 1\}$, representing a small and a large dataset; this will be a baseline in our experiments.

3 Fast Bayesian optimization for large datasets

Here, we introduce our new approach for FAsT Bayesian Optimization on LARge data Sets (FABOLAS). While traditional Bayesian hyperparameter optimizers model the loss of machine learning algorithms on a given dataset as a blackbox function f to be minimized, FABOLAS models loss and computational cost *across dataset size* and uses these models to carry out Bayesian optimization with an extra degree of freedom. The blackbox function $f : \mathbb{X} \times \mathbb{R} \rightarrow \mathbb{R}$ now takes another input representing the data subset size; we will use relative sizes $s \in [0, 1]$, with $s = 1$ representing the entire dataset. While the eventual goal is to minimize the loss $f(\mathbf{x}, s = 1)$ for the entire dataset, evaluating f for smaller s is usually cheaper, and the function values obtained correlate across s . Unfortunately, this correlation structure is unknown initially, so the challenge is to design a strategy that trades off the cost of function evaluations against the benefit of learning about the scaling behavior of f and, ultimately, about which configurations work best on the full dataset. Following the nomenclature of Williams et al. [26], we call $s \in [0, 1]$ an *environmental variable* that can be changed freely *during* optimization, but that is set to $s = 1$ (i.e., the entire dataset size), at evaluation time.

We propose a principled rule for the automatic selection of the next (\mathbf{x}, s) pair to evaluate. In a nutshell, where standard Bayesian optimization would always run configurations on the full dataset, we use ES to reason about, for each size s , how much there is to learn about performance on the full dataset from a test at s . In doing so, FABOLAS automatically determines the amount of data necessary to (usefully) extrapolate to the full dataset.

For an initial intuition on how performance changes with dataset size, we evaluated a grid of 400 configurations of a support vector machine (SVM) on subsets of the MNIST dataset [27]; MNIST has $N = 50\,000$ data points and our subsets had size $N_{\text{sub}} \in \{N/512, N/256, N/128, \dots, N/4, N/2, N\}$. Figure 1 visualizes the validation error of these configurations on subsets of size $N/128$, $N/16$, $N/4$, and N . Evidently, just $1/128$ of the dataset is quite representative and sufficient to locate a reasonable configuration. Additionally, there are no deceiving local optima on smaller subsets. Based on these observations, we expect that relatively small fractions of the dataset are already representative and therefore vary our relative size parameter s on a logarithmic scale: $s = (\log N_{\text{sub}} - \log N_{\text{min}}) / (\log N - \log N_{\text{min}})$, where N_{sub} is the actual number of data points used, with boundaries N_{min} and N .

3.1 Kernels for loss and computational cost

To transfer the insights from this illustrative example into a formal model for the loss and cost across subset sizes, we extend the GP model by an additional input dimension, namely $s \in [0, 1]$. This allows the surrogate to extrapolate to the full data set at $s = 1$ without necessarily evaluating there. We chose a factorized kernel, consisting of the standard stationary kernel over hyperparameters, multiplied with a finite-rank (“degenerate”) covariance function in s :

$$k((\mathbf{x}, s), (\mathbf{x}', s')) = k_{5/2}(\mathbf{x}, \mathbf{x}') \cdot (\phi^T(s) \cdot \Sigma_\phi \cdot \phi(s')). \quad (6)$$

Since any choice of the basis function ϕ yields a positive semi-definite covariance function, this provides a flexible language for prior knowledge relating to s .

We use the same form of kernel to model the loss f and cost c , respectively, but with different basis functions ϕ_f and ϕ_c based on background knowledge. For the former, we exploit that the loss of machine learning algorithms usually decreases with more training data and thus choose $\phi_f(s) = (1, (1-s)^2)^T$ to enforce monotonic predictions with an extremum at $s = 1$. To model the computational cost c , we exploit that complexity usually grows with the number of data points N_{sub} . To allow fitting polynomial complexity $O(N_{\text{sub}}^\alpha)$ for arbitrary α and simultaneously force predictions to be positive, we model the log-cost and use $\phi_c(s) = (1, s)^T$. In the supplemental material (Section B), we visualize scaling of loss and cost with dataset size for the SVM example above and show that our kernels indeed fit them well. We also evaluate the possibility of modelling the heteroscedastic noise introduced by subsampling the data (supplementary material, Section C).

3.2 Formal algorithm description

Algorithm 1 Fast BO for Large Datasets (FABOLAS)

- 1: Initialize data \mathcal{D}_0 using an initial design.
 - 2: **for** $t = 1, 2, \dots$ **do**
 - 3: Fit GP models for $f(\mathbf{x}, s)$ and $c(\mathbf{x}, s)$ on data \mathcal{D}_{t-1}
 - 4: Choose (\mathbf{x}_t, s_t) by maximizing the acquisition function in Equation 7.
 - 5: Evaluate $y_t \sim f(\mathbf{x}_t, s_t) + \mathcal{N}(0, \sigma^2)$, also measuring cost $z_t \sim c(\mathbf{x}_t, s_t) + \mathcal{N}(0, \sigma_c^2)$, and augment the data: $\mathcal{D}_t = \mathcal{D}_{t-1} \cup \{(\mathbf{x}_t, s_t, y_t, z_t)\}$
 - 6: Choose incumbent $\hat{\mathbf{x}}_t$ based on the predicted loss at $s = 1$ of all $\{\mathbf{x}_1, \mathbf{x}_2, \dots, \mathbf{x}_t\}$.
 - 7: **end for**
-

Algorithm 1 lists pseudocode for FABOLAS. We also provide an open-source implementation at <https://github.com/automl/RoboBO>. The algorithm starts with an initial design, described in more detail in Section 3.3. Afterwards, at the start of each iteration it fits GPs for loss and computational cost across dataset sizes s using the kernel from Eq. 6 (line 3). Then, capturing the distribution of the optimum for $s = 1$ using $p_{\min}^{s=1}(\mathbf{x} \mid \mathcal{D}) := p(\mathbf{x} \in \arg \min_{\mathbf{x}' \in \mathbb{X}} f(\mathbf{x}', s=1) \mid \mathcal{D})$, it selects the maximizer of the following acquisition function to trade off information gain versus cost:

$$a_F(\mathbf{x}, s) := \frac{\mathbb{E}_{p(y|\mathbf{x}, s, \mathcal{D})} \left[\int p_{\min}^{s=1}(\mathbf{x}' \mid \mathcal{D} \cup \{(\mathbf{x}, s, y)\}) \cdot \log \frac{p_{\min}^{s=1}(\mathbf{x}' \mid \mathcal{D} \cup \{(\mathbf{x}, s, y)\})}{u(\mathbf{x}')} d\mathbf{x}' \right]}{c(\mathbf{x}, s) + c_{\text{overhead}}}. \quad (7)$$

This acquisition function resembles the one used by MTBO (Eq. 5), with two differences: First, MTBO’s discrete tasks t are replaced by a continuous dataset size s (allowing to learn correlations without evaluations at $s = 1$, and to choose the appropriate subset size automatically). Second, the prediction of computational cost is augmented by the overhead of the Bayesian optimization method. This inclusion of the reasoning overhead is important to appropriately reflect the information gain per unit time spent: it does not matter whether the time is spent with a function evaluation or with reasoning about which evaluation to perform. In practice, due to cubic scaling in the number of data points of GPs and the computational complexity of approximating $p_{\min}^{s=1}$, the additional overhead of FABOLAS is within the order of minutes, such that differences in computational cost in the order of seconds become negligible in comparison.³

³The same is true for standard ES and MTBO, but it was never exploited as no emphasis was put on the total wall clock time spent for the hyperparameter optimization. We emphasize that we express budgets in terms of wall clock time (not in terms of function evaluations) since this is natural in most practical applications.

Being an anytime algorithm, FABOLAS keeps track of its incumbent at each time step (line 6). To select a configuration that performs well on the full dataset, it predicts the loss of all evaluated configurations at $s = 1$ using the GP model and picks the minimizer. We found this to work more robustly than globally minimizing the posterior mean, or similar approaches.

3.3 Initial design

It is common in Bayesian optimization to start with an initial design of points chosen at random or from a Latin hypercube design to allow for reasonable GP models as starting points. To fully leverage the speedups we can obtain from evaluating small datasets, we bias this selection towards points with small (cheap) datasets in order to improve the prediction for dependencies on s : We draw $k = 40$ random points in \mathbb{X} and evaluate 10 each for $N_{\text{sub}} \in \{N/32, N/16, N/8, N/4\}$. This provides information on scaling behavior with s , and, assuming that costs increase linearly or superlinearly with s , these k function evaluations nevertheless cost less than $\frac{k}{8}$ function evaluations at the full dataset size N . This is important since the cost of the initial design of course counts towards FABOLAS’ runtime.

3.4 Implementation details

The presentation of FABOLAS above omits some details that impact the performance of our method. As it has become standard in Bayesian optimization [5], we use Markov-Chain Monte Carlo (MCMC) integration to marginalize over the GPs hyperparameters (we use the emcee package [28]). To accelerate the optimization, we use hyper-priors to emphasize meaningful values for the parameters, chiefly adopting the choices of the SPEARMINT toolbox [5]: a uniform prior between $[-2, 2]$ for all length scales λ in log space, a lognormal prior ($\mu_a = 0, \sigma_a^2 = 1$) for the covariance amplitude θ , and a horseshoe prior with length scale of 0.1 for the noise variance σ^2 .

We used the original formulation of ES by Hennig and Schuler [24] rather than the recent reformulation of PES by Hernández-Lobato et al. [25]. The main reason for this is that the latter prohibits non-stationary kernels due to its use of Bochner’s theorem for a spectral approximation. PES could in principle be extended to work for our particular choice of kernels (using an Eigen-expansion, from which we could sample features); since this would complicate making modifications to our kernel, we leave it as an avenue for future work, but note that in any case it may only further improve our method.

4 Experiments

We present an empirical evaluation of FABOLAS, comparing to standard Bayesian optimization using the acquisition functions EI and ES, and to MTBO. For each method we tracked wall clock time (counting both optimization overhead and the cost of function evaluations, including the initial design), storing the incumbent returned after every iteration. In an offline validation step, we then trained models with all incumbents on the full dataset and measured their test error. We plot these test errors throughout.⁴ Also throughout, to obtain error bars, we performed 10 independent runs of each Bayesian optimization method with different seeds (except on the grid experiment, where we could afford 30 runs per method) and plot medians, along with 25th and 75th percentiles. Details on the hyperparameter ranges used in every experiment are given in the supplemental material (Section D).

4.1 Support vector machine grid on MNIST

First, we considered a benchmark allowing comparison to the ground truth: our SVM grid on MNIST (described in Section 3), for which we had performed all function evaluations beforehand, measuring loss and cost 10 times for each configuration \mathbf{x} and subset size s to account for performance variations. (In this case, we computed each method’s wall clock time in each iteration as its summed optimization overheads so far, plus the summed costs for the function values it queried so far.)

⁴The residual network in Section 4.4 is an exception: here, we trained networks with the incumbents on the full training set (50000 data points, augmented to 100000 as in the original code) and then measured and plotted performance on the validation set.

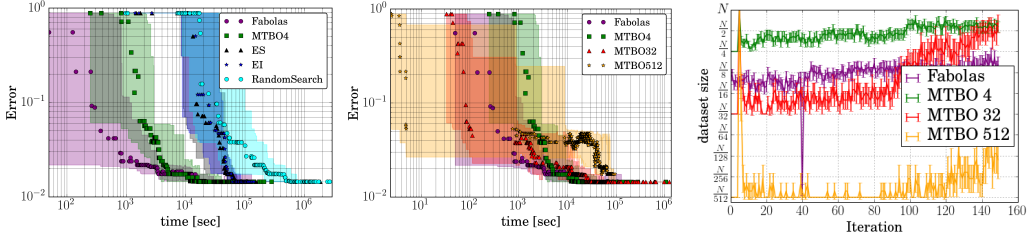


Figure 2: Evaluation on SVM grid on MNIST. (Left) Baseline comparison of test performance of the methods’ selected incumbents over time. (Middle) Test performance over time for variants of MTBO with different dataset sizes for the auxiliary task. (Right) Dataset size FABOLAS and MTBO pick in each iteration to trade off small cost and high information gain; unlike elsewhere in the paper, this right plot shows mean $\pm 1/4$ stddev of 30 runs (medians would only take two values for MTBO).

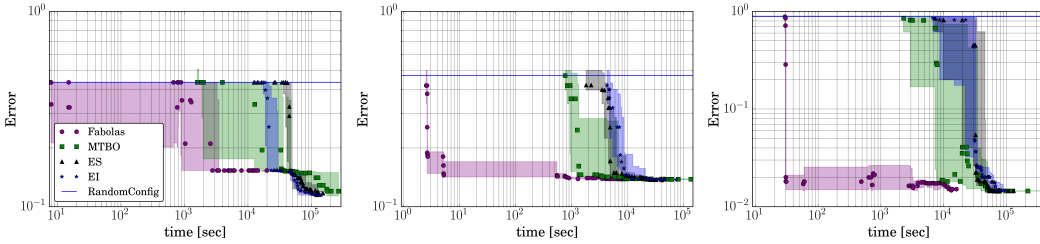


Figure 3: SVM hyperparameter optimization on the datasets coverytype (left), vehicle (middle) and MNIST(right). At each time, the plots show test performance of the methods’ respective incumbents. FABOLAS finds a good configuration between 10 and 1000 times faster than the other methods.

Figure 2 (left) shows results using EI, ES, random search, MTBO and FABOLAS on this SVM benchmark. EI and ES perform equally well and find the best configuration (which yields an error of 0.014, or 1.4%) after around 10^5 seconds, roughly five times faster than random search. MTBO achieves good performance faster, requiring only around 2×10^4 seconds to find the global optimum. FABOLAS is roughly another order of magnitude faster than MTBO in finding good configurations, and finds the global optimum at the same time.

MTBO requires choosing the number of data points in its auxiliary task. At first glance, one may expect that it would work best with many tasks (e.g., with a task for each of $N/512, N/256, \dots, N/4, N/2$, and N), but performance with several tasks is actually poor since with $|T|$ tasks there are $\binom{|T|}{2}$ terms to learn in the discrete task kernel. Better performance can be obtained with only one auxiliary task. Figure 2 (middle) evaluates MTBO variants with a single auxiliary task of $N/4, N/32$, and $N/512$ data points, respectively. With auxiliary tasks at either $N/512$ or $N/32$, MTBO started quickly but took quite long to converge to the optimum; we believe this is because the correlation between the tasks is too small. An auxiliary task size of $N/4$ worked best and we used this for MTBO in the remaining experiments (including in Figure 2 (left) discussed above). We also evaluated MTBO with 3 different auxiliary tasks ($N/4, N/32$, and $N/512$), but found this to perform worse than the variant with only one auxiliary tasks at $N/4$. Figure 2 (right) shows the dataset sizes chosen by the different algorithms during the optimization; all methods slowly increased the average subset size used over time.

4.2 Support vector machines on various datasets

For a more realistic scenario, we optimized the same SVM hyperparameters without a grid constraint on MNIST and two other prominent UCI datasets (vehicle registration [29] and forest cover types [30]) with more than 50000 data points. Training SVMs on these datasets can take several hours, and Figure 3 shows that FABOLAS found good configurations for them between 10 and 1000 times faster than the other methods.

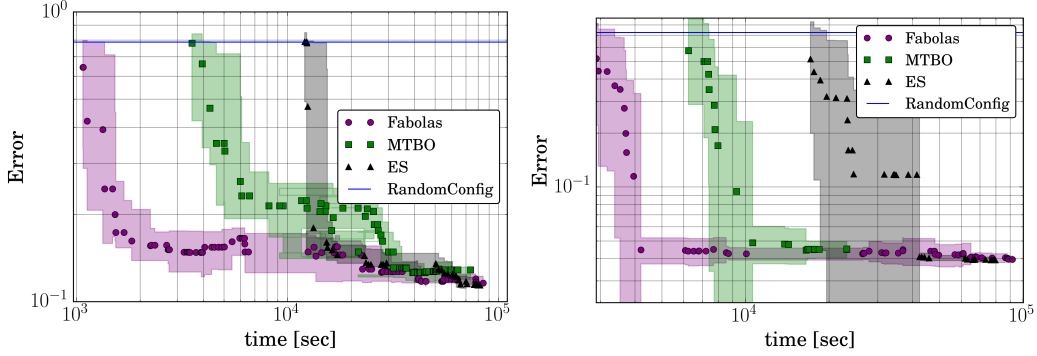


Figure 4: Test performance of a convolutional neural network on CIFAR10 (left) and SVHN (right).

4.3 Convolutional neural networks on CIFAR-10 and SVHN

Convolutional neural networks (CNNs) have shown superior performance on a variety of computer vision and speech recognition benchmarks, but finding good hyperparameter settings is still a challenge, and almost no theoretical guarantees exists. Tuning CNNs for modern large datasets is often infeasible via standard Bayesian optimization; this was in fact our main motivation to develop FABOLAS.

We experimented with hyperparameter optimization for CNNs on the two well-established object recognition datasets CIFAR10 [12] and SVHN [31]. We used the same setup for both datasets (a CNN with four convolutional layers, with dropout [32] in each layer, optimized using Adam [33]). We decayed the learning rate over time and considered a total of six hyperparameters: the initial and the final learning rate and the number of units in each layer. For CIFAR10, we used 45000 images for training, 5000 to estimate validation error, and the standard 10000 hold-out images to estimate the final test performance of incumbents. For SVHN, we used 6000 of the 73257 training images to estimate validation error, the rest for training, and the standard 26032 images for testing.

The results in Figure 4 show that—compared to the SVM tasks—FABOLAS’ speedup was smaller because CNNs only scale linearly in the number of datapoints. Nevertheless it found good configurations about 10 times faster than vanilla Bayesian optimization.

4.4 Residual neural network on CIFAR-10

In the final experiment, we optimized the validation performance of a deep residual network [34] on the CIFAR10 dataset, using the original architecture from [34]. As hyperparameters we exposed the learning rate, L_2 regularization, momentum and the factor that we multiply on the learning rate after 41 and 61 epochs.

Figure 5 shows that FABOLAS found reasonable performance roughly 10 times faster than ES and MTBO and found the optimum at roughly the same time.

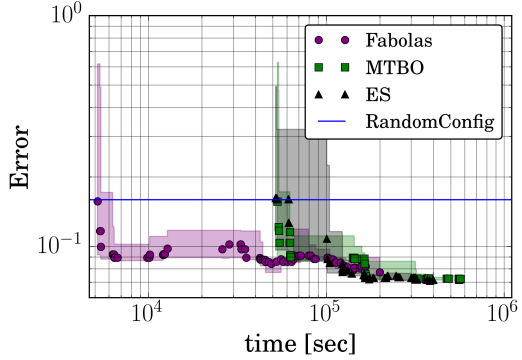


Figure 5: Validation performance of a residual network on CIFAR10.

5 Conclusion

We presented FABOLAS, a new Bayesian optimization method based on entropy search that mimics human experts in evaluating algorithms on subsets of the data to quickly gather information about good hyperparameter settings. FABOLAS extends the standard way of modelling the objective function by treating the dataset size as an additional continuous input variable. This allows the incorporation of strong prior information. FABOLAS additionally models the time it takes to evaluate a configuration and aims to evaluate points that yield—per time spent—the most information about the globally best hyperparameters for the full dataset. In various hyperparameter optimization experiments using

support vector machines and deep neural networks, FABOLAS often found good configurations 10 to 100 times faster than the related approach of Multi-Task Bayesian optimization and standard Bayesian optimization. Our open-source code is available at <https://github.com/automl/RobO>.

In future work, we will expand our algorithm to model other environmental variables, such as the resolution size of images, the number of classes, and the number of epochs, and we expect this to yield additional speedups. Since our method reduces the cost of individual function evaluations but requires more of these cheaper evaluations, we expect that in many practical applications the cubic complexity of Gaussian processes may become the limiting factor and are planning to study whether other model classes, such as Bayesian neural networks [35, 36, 37], may yield similar predictive quality at a lower computational complexity.

References

- [1] G. Montavon, G. Orr, and K.-R. Müller, editors. *Neural Networks: Tricks of the Trade - Second Edition*. LNCS. Springer, 2012.
- [2] J. Bergstra, R. Bardenet, Y. Bengio, and B. Kégl. Algorithms for hyper-parameter optimization. In *Proc. of NIPS'11*, 2011.
- [3] F. Hutter, H. Hoos, and K. Leyton-Brown. Sequential model-based optimization for general algorithm configuration. In *Proc. of LION'11*, 2011.
- [4] J. Bergstra and Y. Bengio. Random search for hyper-parameter optimization. *JMLR*, 2012.
- [5] J. Snoek, H. Larochelle, and R. P. Adams. Practical Bayesian optimization of machine learning algorithms. In *Proc. of NIPS'12*, 2012.
- [6] R. Bardenet, M. Brendel, B. Kégl, and M. Sebag. Collaborative hyperparameter tuning. In *Proc. of ICML'13*, 2013.
- [7] J. Bergstra, D. Yamins, and D. Cox. Making a science of model search: Hyperparameter optimization in hundreds of dimensions for vision architectures. In *Proc. of ICML'13*, 2013.
- [8] K. Swersky, J. Snoek, and R. Adams. Multi-task Bayesian optimization. In *Proc. of NIPS'13*, 2013.
- [9] K. Swersky, J. Snoek, and R. Adams. Freeze-thaw Bayesian optimization. *CoRR*, 2014.
- [10] J. Snoek, K. Swersky, R. Zemel, and R. Adams. Input warping for Bayesian optimization of non-stationary functions. In *Proc. of ICML'14*.
- [11] J. Snoek, O. Rippel, K. Swersky, R. Kiros, N. Satish, N. Sundaram, M. M. A. Patwary, Prabhat, and R. P. Adams. Scalable Bayesian optimization using Deep Neural Networks. In *Proc. of ICML'15*, 2015.
- [12] A. Krizhevsky. Learning multiple layers of features from tiny images. Technical report, University of Toronto, 2009.
- [13] T. Domhan, J. T. Springenberg, and F. Hutter. Speeding up automatic hyperparameter optimization of deep neural networks by extrapolation of learning curves. In *Proc. of IJCAI'15*, 2015.
- [14] L. Bottou. Stochastic gradient tricks. In Grégoire Montavon, Genevieve B. Orr, and Klaus-Robert Müller, editors, *Neural Networks, Tricks of the Trade, Reloaded*. Springer, 2012.
- [15] T. Nickson, M. A Osborne, S. Reece, and S. Roberts. Automated machine learning on big data using stochastic algorithm tuning. *CoRR*, 2014.
- [16] T. Krueger, D. Panknin, and M. Braun. Fast cross-validation via sequential testing. *JMLR*, 2015.
- [17] E. Brochu, V. Cora, and N. de Freitas. A tutorial on Bayesian optimization of expensive cost functions, with application to active user modeling and hierarchical reinforcement learning. *CoRR*, 2010.
- [18] B. Shahriari, K. Swersky, Z. Wang, R. Adams, and N. de Freitas. Taking the human out of the loop: A Review of Bayesian Optimization. *Proc. of the IEEE*, (1), 12/2015 2016.
- [19] C. Rasmussen and C. Williams. *Gaussian Processes for Machine Learning*. The MIT Press, 2006.
- [20] B. Matérn. Spatial variation. *Meddelanden fran Statens Skogsforskningsinstitut*, 1960.
- [21] D.J.C. MacKay and R.M. Neal. Automatic relevance detection for neural networks. Technical report, University of Cambridge, 1994.
- [22] J. Mockus, V. Tiesis, and A. Zilinskas. The application of Bayesian methods for seeking the extremum. *Towards Global Optimization*, (117-129), 1978.
- [23] N. Srinivas, A. Krause, S. Kakade, and M. Seeger. Gaussian process optimization in the bandit setting: No regret and experimental design. In *Proc. of ICML'10*, 2010.
- [24] P. Hennig and C. Schuler. Entropy search for information-efficient global optimization. *JMLR*, (1), 2012.
- [25] J. Hernández-Lobato, M. Hoffman, and Z. Ghahramani. Predictive entropy search for efficient global optimization of black-box functions. In *Proc. of NIPS'14*, 2014.
- [26] B. Williams, T. Santner, and W. Notz. Sequential design of computer experiments to minimize integrated response functions. *Statistica Sinica*, 2000.
- [27] Y. LeCun, L. Bottou, Y. Bengio, and P. Haffner. Gradient-based learning applied to document recognition. In S. Haykin and B. Kosko, editors, *Intelligent Signal Processing*. IEEE Press, 2001.
- [28] D. Foreman-Mackey, D. W. Hogg, D. Lang, and J. Goodman. emcee : The MCMC Hammer. *PASP*, 2013.
- [29] J.P. Siebert. *Vehicle Recognition Using Rule Based Methods*. Turing Institute, 1987.

- [30] J A Blackard and D J Dean. Comparative accuracies of artificial neural networks and discriminant analysis in predicting forest cover types from cartographic variables. *Comput. Electron. Agric.*, 1999.
- [31] Y. Netzer, T. Wang, A. Coates, A. Bissacco, B. Wu, and A. Y. Ng. Reading digits in natural images with unsupervised feature learning. In *NIPS Workshop on Deep Learning and Unsupervised Feature Learning 2011*, 2011.
- [32] N. Srivastava, G. Hinton, A. Krizhevsky, I. Sutskever, and R. Salakhutdinov. Dropout: A simple way to prevent neural networks from overfitting. *Journal of Machine Learning Research*, 2014.
- [33] D. P. Kingma and J. Ba. Adam: A method for stochastic optimization. *CoRR*, 2014.
- [34] K. He, X. Zhang, S. Ren, and J. Sun. Deep residual learning for image recognition. *CoRR*, 2015.
- [35] R. Neal. Bayesian learning for neural networks. *PhD thesis, University of Toronto*, 1996.
- [36] J. Hernández-Lobato and R. Adams. Probabilistic backpropagation for scalable learning of bayesian neural networks. In *Proc. of ICML'15*, 2015.
- [37] C. Blundell, J. Cornebise, K. Kavukcuoglu, and D. Wierstra. Weight uncertainty in neural networks. In *Proc. of ICML'15*, 2015.
- [38] Thomas P. Minka. Expectation propagation for approximate bayesian inference. In *Proc. of UAI'01*, UAI '01, San Francisco, CA, USA, 2001. Morgan Kaufmann Publishers Inc.
- [39] J. Cunningham, P. Hennig, and S. Lacoste-Julien. Approximate gaussian integration using expectation propagation. pages 1–11, January 2012.
- [40] Peter Sollich. Gaussian process regression with mismatched models. In T.G. Dietterich, S. Becker, and Z. Ghahramani, editors, *Advances in Neural Information Processing Systems 14*. MIT Press, 2002.

A Entropy Search

A.1 Approximations used

Given $p(f)$, the probability that a point is the minimum is defined with suggestive notation as

$$p_{\min}(\mathbf{x}|\mathcal{D}) = p(\mathbf{x} = \arg \min_{\mathbf{x}' \in \mathcal{X}} f(\mathbf{x}')|D) = \int p(f|\mathcal{D}) \prod_{\substack{\tilde{\mathbf{x}} \in [a,b] \\ \tilde{\mathbf{x}} \neq \mathbf{x}}} \Theta[f(\tilde{\mathbf{x}}) - f(\mathbf{x})] df \quad (8)$$

where Θ is Heaviside's step function. The product in this equation is over an infinite domain (yet well-defined if $p(f|D)$ is sufficiently regular). In practice, it has to be represented in a finite form. We follow the approach of Hennig and Schuler [24], who approximate $p(f|D)$ by a finite-dimensional Gaussian over an irregular grid of points $\mathbf{r}_1, \dots, \mathbf{r}_Z$, which are designed heuristically to provide good interpolation resolution on p_{\min} . Like Hennig and Schuler [24], we sample these so called representer points using Expected Improvement. This step reduces p_{\min} to a discrete distribution, and turns the infinite product in Equation 8 into a finite one. That distribution itself is still analytically intractable, but an analytically tractable (in particular, differentiable) approximation $q_{\min}(\mathbf{r}_j)$ of good empirical quality can be computed using *Expectation Propagation (EP)* [38], at computational cost in $\mathcal{O}(Z^4)$. EP does not only yield p_{\min} , but also the gradient with respect to means and covariances of the model at the representer points allowing efficient computations after an expensive initial calculation of these quantities. This particular application of EP to Gaussian integrals was introduced by Cunningham et al. [39] where all the details can be found.

A.2 Pseudocode

Algorithm 2 provides pseudocode for our implementation of Entropy Search. Lines 1-12 precompute various quantities that are needed for evaluating the acquisition function, which is optimized in line 13. Specifically, after sampling K hyperparameter settings from the marginal loglikelihood for the GP using MCMC (line 1), for every hyperparameter setting θ_i , the algorithm

- fits a GP (line 4),
- samples representer points with respect to a_{EI} (line 5),
- stores the representer points and their logarithmic EI values (lines 6 and 7),
- computes $\boldsymbol{\mu}$ and Σ for the joint predictive distribution at the representer points (line 8),
- computes p_{\min} given $\boldsymbol{\mu}$ and Σ , using EPMGP (line 9),
- draws random points from a normal distribution centered at 0 and unit variance (line 10) for the innovation in Algorithm 4, and stores them (line 11) for later usage.

Algorithm 2 Selection of next point by Entropy Search

Require: $\mathcal{D}_n = (\mathbf{x}_j, y_j)_{j=1 \dots n}$

- 1: Sample K instantiations of the GP hyperparameters $\Theta = [\theta_1, \dots, \theta_K]$ w.r.t. marginal likelihood
 - 2: $p_{\min} \leftarrow [], \Omega \leftarrow [], \mathbf{R} \leftarrow [], \mathbf{U} \leftarrow []$
 - 3: **for** $i = 1 \dots K$ **do**
 - 4: Fit GP model $\mathcal{M}^{(i)}$ on \mathcal{D}_n with hyperparameter θ_i
 - 5: $(\mathbf{r}_1, a_{EI}(\mathbf{r}_1)) \dots, (\mathbf{r}_Z, a_{EI}(\mathbf{r}_Z)) \sim a_{EI}(\mathbf{x}|\mathcal{M}^{(i)})$ ▷ Sample Z representer points
 - 6: $\mathbf{R}[i] \leftarrow \mathbf{r}_1, \dots, \mathbf{r}_Z$ ▷ Store representer points $\mathbf{R} \in \mathbb{R}^{K \times Z \times D}$
 - 7: $\mathbf{U}[i] \leftarrow a_{EI}(\mathbf{r}_1), \dots, a_{EI}(\mathbf{r}_Z)$ ▷ Store LogEI values of the representer points $\mathbf{U} \in \mathbb{R}^{K \times Z}$
 - 8: Let $\boldsymbol{\mu}, \Sigma$ be the mean and covariance matrix at $\mathbf{r}_1, \dots, \mathbf{r}_Z$ based on $\mathcal{M}^{(i)}$
 - 9: $p_{\min}[i] \leftarrow \text{computePmin}(\boldsymbol{\mu}, \Sigma)$ ▷ Probability of each $\mathbf{r}_1, \dots, \mathbf{r}_Z$ to be the minimum.
 - 10: For $p = 1, \dots, P$: $\boldsymbol{\omega}_p \sim \mathcal{N}(0, \mathbf{I}_Z)$ ▷ Stochastic change to hallucinate P values at representer points
 - 11: $\Omega[i] \leftarrow [\boldsymbol{\omega}_1, \dots, \boldsymbol{\omega}_P]$ ▷ Store stochastic change for the innovations $\Omega \in \mathbb{R}^{K \times Z \times P}$
 - 12: **end for**
 - 13: $\mathbf{x}_{n+1} \leftarrow \arg \max_{\mathbf{x} \in \mathcal{X}} \text{InformationGain}(\mathbf{x}, \mathcal{D}_n, \mathbf{R}, \mathbf{U}, \Omega, \Theta)$
 - 14: **return** \mathbf{x}_{n+1}
-

Given these quantities, Algorithm 3 then computes the ES acquisition function from Equation (3) in the main paper (repeated here for convenience):

$$a_{\text{ES}}(\mathbf{x}) := \mathbb{E}_{p(y|\mathbf{x}, \mathcal{D})} \left[\int p_{\min}(\mathbf{x}' | \mathcal{D} \cup \{(\mathbf{x}, y)\}) \cdot \log \frac{p_{\min}(\mathbf{x}' | \mathcal{D} \cup \{(\mathbf{x}, y)\})}{u(\mathbf{x}')} d\mathbf{x}' \right].$$

For each hyperparameter θ_i of the GP, it then carries out the following steps:

- train a model $\mathcal{M}^{(i)}$ on the data \mathcal{D} by computing the Cholesky decomposition (line 3)
- based on this model $\mathcal{M}^{(i)}$, compute the mean and the variance for the test point \mathbf{x} and the mean and covariance for the representer points $\mathbf{r}_1, \dots, \mathbf{r}_Z$ (line 4 and 5)
- For each of the P stochastic change vectors ω_p sampled in Algorithm 1 (line 10) and stored in $\Omega[i, j, :]$,
 - fantasize the change $\Delta\mu, \Delta\Sigma$ of the current posterior $p(f|D)$ (line 7) with Algorithm 4
 - estimate the p_{\min} distribution of this updated posterior (line 8)
 - compute the relative change in entropy (line 9)
- take the expectation over $p(y|\mathbf{x}, D)$ of Equation (3) (line 10)
- marginalize the acquisition function $a_{\text{ES}}(\mathbf{x})$ over all hyperparameters Θ (line 13)

Algorithm 3 InformationGain

Require: $\mathbf{x}, \mathcal{D}, \mathbf{R}, \mathbf{U}, \Omega, \Theta$

```

1:  $a(\mathbf{x}) \leftarrow 0$ 
2: for  $i = 1, \dots, K$  do ▷ Marginalization over  $\Theta$ 
3:   Let  $\mathcal{M}^{(i)}$  be the trained model on  $\mathcal{D}$  with hyperparameters  $\theta_i$ 
4:   Let  $\mu, \sigma^2$  be the predictive mean and variance at  $\mathbf{x}$  based on  $\mathcal{M}^{(i)}$ 
5:   Let  $\mu, \Sigma$  be the mean and covariance matrix at  $\mathbf{r}_1, \dots, \mathbf{r}_Z$  based on  $\mathcal{M}^{(i)}$ 
6:   for  $j = 0, \dots, P$  do ▷ Averages over all hallucinated values.
7:      $\Delta\mu, \Delta\Sigma \leftarrow \text{Innovations}(\mathbf{x}, \mathcal{M}^{(i)}, \mathbf{R}[i, :, :], \sigma^2, \Omega[i, j, :])$  ▷ Change in the posterior
       believe at  $\mathbf{r}_1, \dots, \mathbf{r}_Z$  if we would evaluate at  $\mathbf{x}$ 
8:      $q_{\min} \leftarrow \text{computePmin}(\mu + \Delta\mu, \Sigma + \Delta\Sigma)$  ▷ New Pmin of the updated posterior
9:      $dH \leftarrow -\sum_j q_{\min} (\log(q_{\min}) + \mathbf{U}[i]) + \sum_j p_{\min}[i] (\log(p_{\min}[i]) + \mathbf{U}[i])$ 
10:     $a(\mathbf{x}) \leftarrow a(\mathbf{x}) + \frac{1}{P} dH$ 
11:   end for
12: end for
13: return  $\frac{1}{K} a(\mathbf{x})$ 

```

This algorithm in turns makes use of Algorithm 4 to compute the innovations, which

- computes the change in the mean $\Delta\mu$ by first computing the correlation $\Sigma(\mathbf{x}, \mathbf{r})$ of \mathbf{x} and the representer points $\mathbf{r}_1, \dots, \mathbf{r}_Z$ and multiplying it with the Cholesky decomposition of the $k(\mathbf{x}, \mathbf{x})$ and the vector $\omega \in \Omega$. Note that this change is stochastic (line 1).
- computes the change of the covariance (line 2) which is deterministic

Algorithm 4 Innovations

Require: $\mathbf{x}, \mathcal{M}, \mathbf{r}_1, \dots, \mathbf{r}_Z, \sigma^2, \omega$

```

1:  $\Delta\mu(\mathbf{x}) = \Sigma(\mathbf{x}, \mathbf{r}) * \sigma^2 * C[\sigma^2 + \sigma_{\text{noise}}^2] \omega$  ▷  $\Sigma(\mathbf{x}, \mathbf{x}')$  denotes the correlation between  $\mathbf{x}$  and  $\mathbf{x}'$ 
   based on  $\mathcal{M}$ 
2:  $\Delta\Sigma(\mathbf{x}) = \Sigma(\mathbf{x}, \mathbf{r}) * \sigma^2 * \Sigma(\mathbf{x}, \mathbf{r})^T$ 
3: return  $\Delta\mu(\mathbf{x}), \Delta\Sigma(\mathbf{x})$ 

```

B Scaling of Loss and Computational Cost With Dataset Size

The runtime of machine learning algorithms usually scales polynomially with the number of data points (N_{sub}), i.e. $\mathcal{O}(N_{\text{sub}}^\alpha)$ for some positive α . While the computational cost of training grows, the loss of machine learning methods usually decreases with the number of training samples. The computational cost is often largely independent of the hyperparameter values, but the loss depends crucially on the hyperparameter values (which is the reason we want to optimize hyperparameters in the first place).

We invested these trends using our 20×20 grid of SVM configurations for MNIST described in the main text. Figure 6 shows these trends for ten random configurations, evaluated on subsets of different sizes. We note that, as training size increases, the loss of many configurations decreases, but the relative ordering does not change dramatically, such that training on few data points provides information about the full data set. The training time behaves similarly across different configurations. Please note that the complexity of the underlying SVM is not trivial, which is why the curves are not straight lines.

To show that our method, i.e. the kernel we use and our initial design, actually capture these trends, we sampled points from that data as our initial design and predicted loss and cost of unseen configurations, see Figure 7. The cost model already quite accurately captures the growth trends based on this small amount of initial data. The loss model predicts worse (especially for configurations very different from the ones in the initial design), but it also reflects that errors decrease with increasing data set size.

C Modeling the Heteroscedastic Noise

When making the subset size a parameter, we shuffle the data before an evaluation to prevent bias incurred by repeatedly using the same subset. This shuffling introduces additional noise which could be particularly high for small subsets. To investigate this, we again used the SVM grid of 400 configurations from the main paper. We repeated each run with a given subset size $K = 10$ times using different subsets, and estimate the observation noise variance at each point as:

$$\sigma_{\text{obs}}^2(\mathbf{x}_j, s_i) = \frac{1}{K} \sum_{k=1}^K (y_k(\mathbf{x}_j, s_i) - \mu_{i,j})^2, \quad (9)$$

where $\mu_{i,j} = K^{-1} \sum_{k=1}^K y_k(\mathbf{x}_j, s_i)$. The red points in Figure 8 show the mean and standard deviation of $\sigma_{\text{obs}}^2(\mathbf{x}_j, s_i)$ over all configurations for all s_i values considered. As expected, the noise decreases with an increasing s , to a point where σ_{obs}^2 is zero for $s = 1$.

In contrast to this heteroscedastic noise intrinsic to the random subsampling, the commonly used noise hyperparameter σ^2 of a GP (call it σ_{GP}^2) is fixed and typically estimated using MCMC sampling. To compare these two noise values, for each fixed size s , we also trained a GP to predict losses and plotted its estimates σ_{GP}^2 as blue markers in Figure 8. To obtain a good estimate of the GP's hyperparameters, we used a relatively long MCMC chain compared to the ones used during Bayesian optimization. Figure 8 clearly shows that the estimated variance σ_{GP}^2 is always larger than the observation noise σ_{obs}^2 . This might indicate a certain misfit between the true objective and the space of functions the GP can model [40]. Consequently, we believe the heteroscedastic noise from subsampling the data to often be negligible compared to the noise estimated by the MCMC sampling.

Nonetheless, we model the noise decreasing in s by an additive kernel $K_{\text{noise}} = \text{diag}(r_i)$ with $r_i = \alpha s_i^\beta$ for each data point (\mathbf{x}_i, s_i) . This adds a heteroscedastic noise to the Gram matrix of our kernel k_f for our objective function, and we treat α and β as additional hyperparameters. These are marginalized together with the other GP's hyperparameter by sampling from the marginal loglikelihood (see Section 3.4 in the main paper for details). Figure 9 shows sample functions of this kernel for different α and β sampled from their respective priors:

$$\alpha \sim \log \mathcal{N}(-3, 1) \quad \beta \sim \log \mathcal{N}(3, 1). \quad (10)$$

These are not very strong priors, but they still enforce the MCMC sampler to choose configurations similar to those shown in Figure 9, which resemble the ones in Figure 8. We performed preliminary

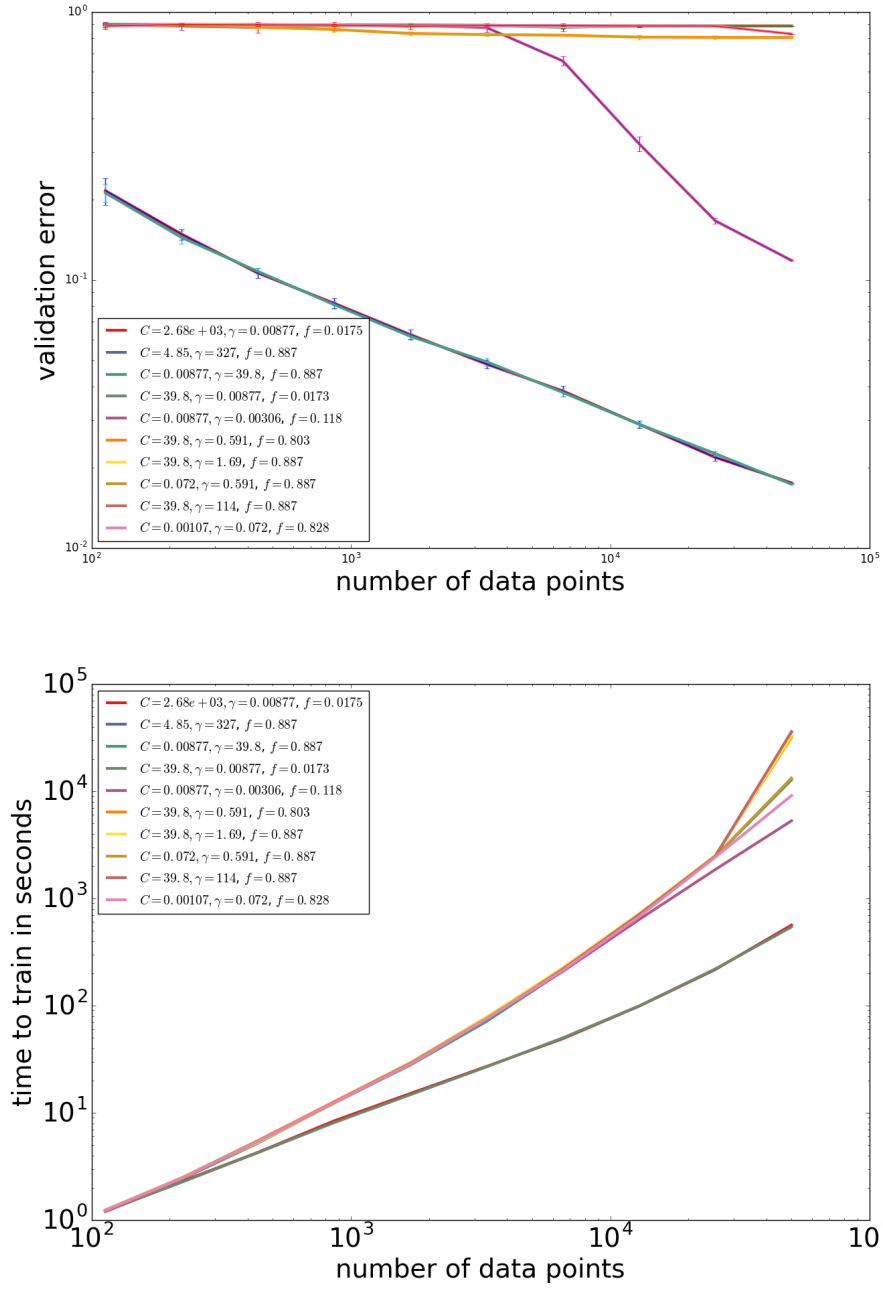


Figure 6: Validation error (left) and training time (left) for ten random configurations training a SVM on the MNIST dataset. For all costs, the cost increases with s whereas the validation error decreases or stays constant.

Bayesian optimization experiments with this kernel, but these did not lead to an additional improvement. We thus we did not use them in our production experiments in order to reduce our model's total number of hyperparameters.

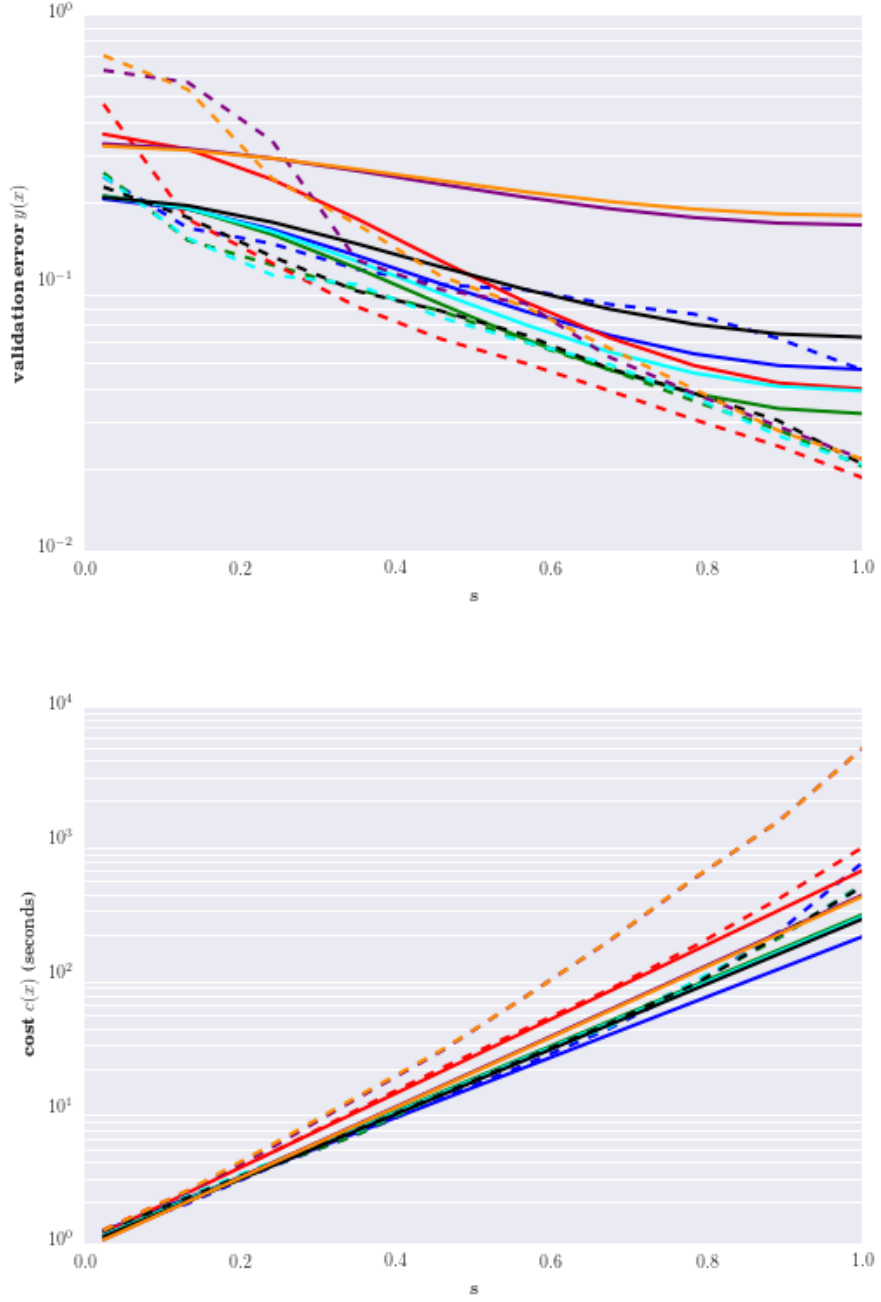


Figure 7: Model (solid line) of the objective function and the cost function (dashed) after the initial design (2 configurations evaluated on $N/16, N/32, N/64, N/128, \frac{N}{256}, N/512$).

D Optimization ranges for Bayesian optimization experiments

Table 1 shows the ranges of the 2 hyperparameters we optimized in our SVM experiments, Table 2 the ranges of the 6 convolutional neural network hyperparameters we optimized, and Table 3 the ranges of the 4 deep residual network hyperparameters we optimized.

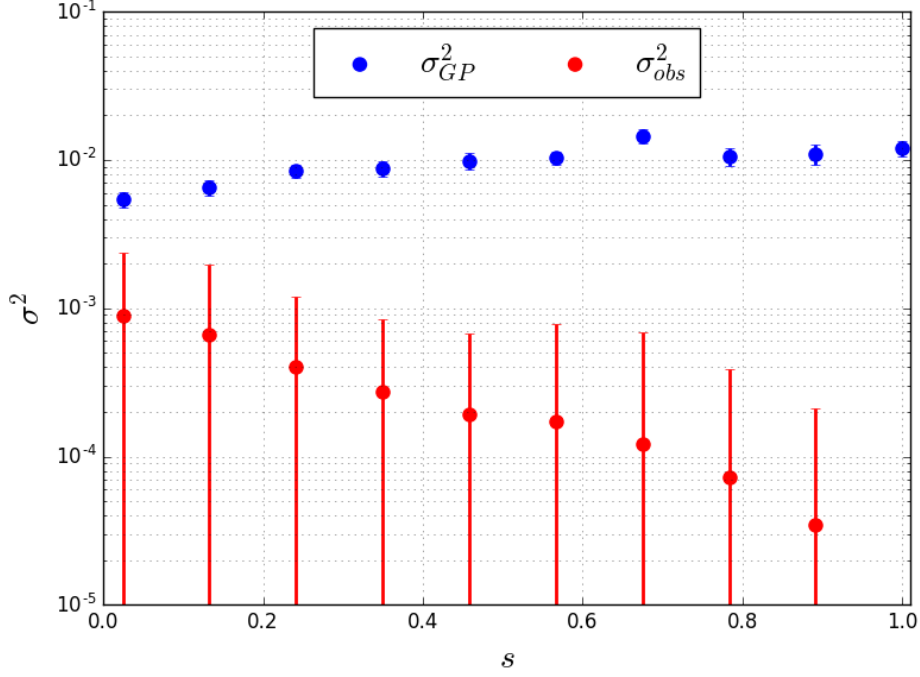


Figure 8: Evaluating a configurations on a shuffled subset of the data induces an additional noise, σ_{obs}^2 that depends on the dataset size s . The noise parameter σ_{GP}^2 estimated by MCMC sampling for fixed dataset sizes.

Table 1: Hyperparameters for all support vector machine tasks.

Hyperparameter	lower bound	upper bound	log
Regularization parameter C	10^{-10}	10^{10}	X
Kernel parameter γ	10^{-10}	10^{10}	X

Table 2: Hyperparameters for the convolutional neural network task.

Hyperparameter	lower bound	upper bound	log
Initial learning rate	10^{-7}	10^{-1}	X
Final learning rate	10^{-3}	10^{-12}	X
# units layer 1	2^3	2^8	X
# units layer 2	2^3	2^8	X
# units layer 3	2^4	2^9	X
# units layer 4	2^4	2^9	X

Table 3: Hyperparameters for the deep residual network task.

Hyperparameter	lower bound	upper bound	log
Learning rate	10^{-6}	1	X
L_2 regularization	10^{-6}	1	X
Learning rate factor	10^{-4}	1	X
Momentum	0.1	0.999	

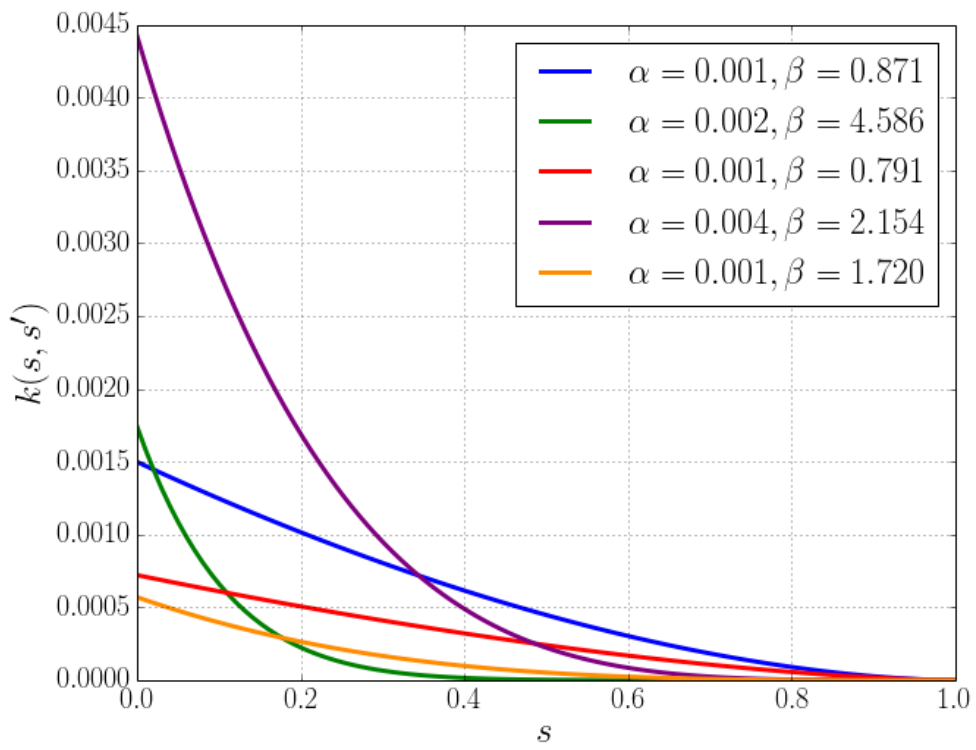


Figure 9: Sample functions of our heteroscedastic noise kernel for different values for its hyperparameters α and β .